ELSEVIER

Chemical Geology 235 (2006) 238–249

CHEMICAL GEOLOGY
INCLUDING
ISOTOPE GEOSCIENCE

www.elsevier.com/locate/chemgeo

In situ stable isotope analysis ($\delta^{13}C$, $\delta^{18}O$) of very small teeth using laser ablation GC/IRMS

Benjamin H. Passey [a,*], Thure E. Cerling [a,b]

[a] *Department of Geology and Geophysics, University of Utah, Salt Lake City, UT 84112, United States*
[b] *Department of Biology, University of Utah, Salt Lake City, UT 84112, United States*

Received 3 July 2006; received in revised form 13 July 2006; accepted 18 July 2006

Editor: P. Deines

Abstract

Current analytical methods for stable isotope analysis of tooth enamel are either destructive to small samples, or require a large amount of material, thereby prohibiting the analysis of very small teeth. This paper describes a number of improvements to thermal laser ablation methods that allow for in situ determination of $\delta^{13}C$ and $\delta^{18}O$ from tooth enamel as thin as 100 μm, representing nearly an order of magnitude decrease in ablation pit depth and volume, and enabling routine enamel-only analysis of small taxa such as rodents. We show that large teeth such as ungulate molars are problematic for this method because they have large CO_2 blanks and cause isotopic fractionation of sample CO_2 related to gas–surface interactions. Isotopic enrichment factors between laser and conventional phosphoric acid method isotope ratios are $^{13}\varepsilon*_{\text{laser-acid}} = -0.3 \pm 1.1‰$ and $-0.5 \pm 0.8‰$ (1σ, modern and fossil samples, respectively), and $^{18}\varepsilon*_{\text{laser-acid}} = -6.4 \pm 0.7‰$ and $-5.1 \pm 1.2‰$. The utility of the method is demonstrated by detailed intra-tooth analyses of rodent and lagomorph incisors that reveal seasonal and other temporal variation in animal isotopic composition. The level of accuracy and precision is sufficient for application to many ecological and paleoenvironmental questions, including reconstruction of the dietary fraction of C_3 versus C_4 vegetation. The accuracy of oxygen isotope analyses is lower than that of conventional methods and some other laser methods, and though large-scale patterns are resolvable, the method is not ideal for applications requiring the highest possible accuracy.

Keywords: Enamel; Laser ablation; Paleoecology; Stable isotope; Fossil teeth

1. Introduction

Stable isotope analysis of tooth enamel is widely used for determining dietary preferences, ecological environment, and (paleo)climatic settings of modern and fossil mammals (Koch, 1998; Kohn and Cerling, 2002). Conventional methods for isotopic analysis of bioapatite include phosphoric acid digestion for the analysis of $\delta^{13}C$ and $\delta^{18}O$ of the carbonate component of bioapatite (McCrea, 1950; Land et al., 1980), and fluorination (Longinelli, 1984; Vennemann et al., 2002) or high temperature reduction (O'Neil et al., 1994; Vennemann et al., 2002; Lecuyer, 2004) of phosphate salts isolated from bioapatite for analysis of $\delta^{18}O$ of the phosphate component. These typically require an initial sample of several milligrams of powdered enamel. The bulk density of pristine enamel is approximately 2.6 mg/mm^3, so the volume of material required for a single isotopic analysis is on the order of several mm^3. This large sample size

* Corresponding author. Fax: +1 801 581 7065.
E-mail address: passey@earth.utah.edu (B.H. Passey).

0009-2541/$ - see front matter © 2006 Elsevier B.V. All rights reserved.
doi:10.1016/j.chemgeo.2006.07.002

requirement is inappropriate for many precious museum specimens, fragile specimens that are destroyed by the drilling necessary to remove samples, and very small teeth. The large sample size requirement has resulted in the disproportionate representation of large, thick-enameled (~1 mm thick or greater) mammals in the isotopic literature. Teeth of smaller mammals such as rodents are abundantly preserved in the fossil record, and the analysis of these along with precious specimens would add significantly to our understanding of past environments.

This paper describes new modifications to thermal ablation techniques that allow rapid and precise carbon and oxygen isotopic determinations on rodent-size teeth with enamel as thin as 100 μm. The methods described here are based on the thermal laser ablation methodologies described by Cerling and Sharp (1996) and Sharp and Cerling (1996). Those methods demonstrated the possibility of in situ analysis of enamel, but have been of little practical use for in situ analysis because laser ablation pit sizes are too large for application to small teeth. They are suitable for large teeth (e.g. Sharp and Cerling, 1998), but large teeth can be more precisely and accurately analyzed using conventional (non-laser) methods. Associated with a reduction in sample size, we identify and mitigate a number of problems that become important when analyzing very small amounts of gas, in particular those relating to sample outgassing, and gas/surface fractionation effects. We demonstrate that reliable in-situ analysis can be performed on small teeth such as rodent and lagomorph incisors, which opens the door to a host of new stable isotope applications in small mammals. We also show, for the first time, that modern tooth enamel can be analyzed using thermal ablation methods, enabling biological applications of stable isotopes in small teeth. Aside from the creation of several small ablation pits per single analysis, this method is non-destructive and is suitable for analyzing small precious teeth and fragile specimens.

This paper does not address other laser-based analytical methodologies, including laser fluorination (Kohn et al., 1996; Jones et al., 1999) and direct laser fluorination (Lindars et al., 2001). Those methods target oxygen isotopes specifically (either from bulk enamel (Kohn et al., 1996; Jones et al., 1999) or CO_3-free enamel (Lindars et al., 2001)), seek high accuracy and precision, and variously require that enamel samples be removed from the teeth prior to analysis (Kohn et al., 1996; Lindars et al., 2001; Grimes et al., 2003) or whole teeth be coated in gold to prevent side reactions in the highly corrosive reaction atmosphere (Jones et al., 1999). The method presented here, thermal laser ablation, differs in that it is capable of measuring both carbon and oxygen isotopes, and that the focus is on in situ, minimally destructive analysis with sufficient accuracy and precision for many but not all applications.

2. Methods

The laser extraction line at the University of Utah is based on the design shown in Fig. 3B of Sharp and Cerling (1996) and Fig. 4 of Sharp et al. (2000), and the general analytical procedure follows the methods described therein for the cryofocusing microcapillary GC method. The key improvement here is a reduction in laser-ablation pit size, primarily in terms of depth, which allows teeth with very thin enamel to be analyzed. This is accomplished using very short duration (~8.5 ms), low power (5–15 W), CO_2 laser radiation (wavelength 10.6 μm), and pooling gas generated from several (~2–8) ablation events for each isotopic determination. Accompanying the small physical sample size is a correspondingly small amount of CO_2 analyzed, which means that background CO_2 contamination and surface–CO_2 interactions become important. There is no discussion of background CO_2 contamination or surface–CO_2 interactions in Cerling and Sharp (1996) or Sharp and Cerling (1996, 1998). We investigate these here and find them to be major problems for some samples, and problems that must be accounted for in the normalization of all data. Therefore, an important aspect of this paper is the methodology and methodological verification necessary to successfully extract small amounts of gas from the sample chamber environment. These include an examination of cryogenic trapping efficiency (Section 3.1), study of the effect of laser power and duration on stable isotope ratios (Section 3.2), analysis of surface–CO_2 interactions that can adsorb and fractionate sample CO_2 (Section 3.1), and identification of sample outgassing and samples that are appropriate or inappropriate for laser ablation analysis (Section 3.1).

Hardware and method specifics are briefly outlined here. In addition to using a sample chamber of the design shown in Cerling and Sharp (1996), we utilize a new design illustrated in Fig. 1 of this paper that allows improved mounting and positioning flexibility, including sample rotation. Rotation is critical for analyzing intra-tooth variation in curved teeth such as rodent incisors, which otherwise would be impossible to analyze without having open the system to successively reposition the sample so that the surface to be analyzed remains normal to the laser beam. Roma plastilina modeling clay is used to fix the samples into position. The extraction line includes septum injection ports located

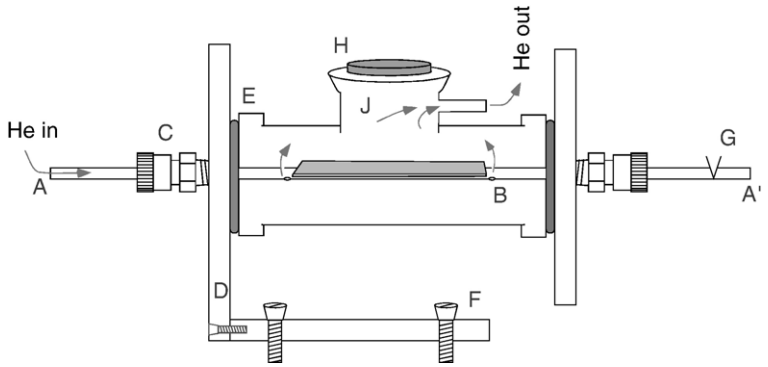

Fig. 1. Feed-through-type sample chamber developed for this study. Samples are mounted on a rotatable and translatable feed through (A-A′) that also serves as a conduit through which helium is introduced into the chamber. The feed-through is 1/4″ stainless steel, and helium enters the chamber through small holes drilled in the tube (B). A tight seal is maintained on the feed-through using bored-through Swagelok® Ultra-Torr® to NPT-threaded union fittings (C), and the glass sample chamber is sealed against aluminum plates (D) using Ace Glass® face-seal o-ring fittings (E) and clamps (not shown). The entire assembly is bolted (F) to a computer-controlled *x–y–z* stage (not shown). A valve (G) allows the dead space of the feed-through to be purged with helium following sample loading. Laser radiation enters the chamber through a ZnSe window (H) that is fixed to the chamber using Apiezon W® 'black wax'. When a sample is ablated by the laser, CO_2 enters the small region of the chamber indicated by (J) and quickly exits via the 'He out' port. Therefore, the effective volume of the chamber from the perspective of laser-generated CO_2 is much smaller than the total chamber volume, which greatly aids rapid and efficient removal of the CO_2 from the chamber.

both upstream and downstream of the sample chamber. The cryogenic trap is a single coil of 1/16″ o.d., 1/25″ i.d. stainless steel tubing, with a total length of 70 cm. The system uses a 25 m, 0.32 mm i.d. Poraplot-Q® GC column (Varian) held at 60 °C, coupled to a Finnigan MAT 252 mass spectrometer by way of a Finnigan GP® open-split interface. The efficiency of the open split is approximately 5:1 (five parts of sample are lost to every one part that enters the mass spectrometer), and the appropriate CO_2 sample size is 10 to 30 nmol. The laser, computer-controlled *x–y–z* stage, and visualization equipment is the MIR 30® system (Merchantek; now New Wave Research). The laser is a CO_2 laser that emits radiation at ~10.6 μm and is rated at 30 W. During the time-period of this study, the laser radiation was measured at a maximum power of 21 W after passing through the focusing lenses. Analyses are carried out with 8.5 ms laser pulse durations in the 5–15 W range, in which there is little or no effect of power on observed isotope ratios (Section 3.2).

For in-situ stable isotope work, a solid-phase international standard is lacking. In order to standardize isotopic data, we utilize internal CO_2 gas standards calibrated against NBS-19 gas produced by reaction with 100% H_3PO_4 at 25 °C in offline sealed vessels. These internal standards are diluted to consist of 3% CO_2 in a balance of UHP N_2, and are injected through the upstream and downstream injection ports on the extraction line. Otherwise these are extracted in exactly the same manner as laser-generated CO_2. Blank determinations are made several times during an analytical run, and data are corrected for background CO_2 contamination using a mass-balance approach. The sequence of applied corrections is blank correction followed by normalization to the upstream-injected CO_2 standard. The upstream standard flows through the entire sample chamber and therefore has a journey most similar to the laser-generated CO_2, which importantly includes exposure to tooth samples in the laser chamber. As an additional quality control measure, we routinely analyze, along with unknown samples, pieces of enamel whose isotopic compositions have been determined in our lab using the phosphoric acid method.

Conventional phosphoric acid analyses were made using a Finnigan Carboflo® common acid bath device coupled to a Finnigan MAT 252 mass spectrometer. The acid temperature was 90 °C, and corrections were made for the temperature dependent oxygen isotope fractionation between CO_2 and mineral using apparent fractionation factors for tooth enamel. Laser ablation pit morphology (depth, width, volume) was determined using scanning electron microscopy and X-ray micro computed tomography, and the digital results of the latter were quantified using the ImageJ software application (National Institutes of Health). CO_2 yields per volume of ablated enamel are expressed as a fraction of the total amount of CO_2 contained in pristine enamel (as CO_3^{2-}). The total amount for the sample studied (K00-AB-302p4.2; modern rhinoceros enamel) was calculated as 1400 nmol/mm^3, which is the product of the weight percent CO_3^{2-} (3.3%), and the bulk density of the enamel (2.6 g/cc).

3. Results

3.1. Cryogenic trapping, blanks, and CO_2–surface interactions

The installation of injection ports on the laser extraction manifold allowed us to quantify cryogenic trapping efficiency by injecting known quantities of CO_2 into the system. We found that trapping efficiency at the high flow rates (up to 250 ml/min) necessary to purge large sample chambers in a timely manner can be less than 50% when the trapping dewar is completely full of liquid nitrogen. This inefficiency in trapping is accompanied by significant isotopic fractionation (usually <0.5‰, but up to 1‰ for both carbon and oxygen). Trapping efficiency is maximized (>90%) when the level of nitrogen is several centimeters below the rim of the dewar. We hypothesize that this relates to thermal gradients seen by the incoming CO_2–helium mixture: when the dewar is full, the thermal gradient is sharp from room temperature to liquid nitrogen temperature, and CO_2 may solidify into particles that pass completely through the trap. When the thermal gradient is lower (i.e. partially full dewar), the CO_2 cannot freeze in midstream, but rather freezes on to the inside walls of the trap and is therefore retained. Regardless of the mechanisms controlling trapping efficiency, it is important to characterize and maximize the trapping efficiency of each hardware/flow rate configuration by means of injecting known quantities of CO_2 into the system.

All samples outgassed significant quantities of CO_2 during the first few hours following loading into the sample chamber, and this is illustrated by way of example for three representative teeth in Fig. 2. Following overnight He purging in the sample chamber, the rate of CO_2 offgassing from several rodent-size teeth is usually low enough to begin analysis (<~1 nmol per single cryogenic-trapping period). In contrast, large teeth such as ungulate molars, and those with large amounts of attached bone or sediment matrix, typically outgassed as much or more CO_2 (>100 nmol) than is generated during a typical laser-ablation analysis event (~10–30 nmol), even after overnight purging.

In attempts to mitigate the CO_2 outgassing problem associated with large samples, we experimented with evacuating samples at elevated temperature (~95 °C) and repeatedly backfilling and re-evacuating the samples with inert gases (Ar, N_2, He). In all cases this led to significant reductions in the rate of CO_2 outgassing and therefore the purging time required before beginning analysis. In most cases, however, samples requiring such treatment ultimately gave poor isotopic results,

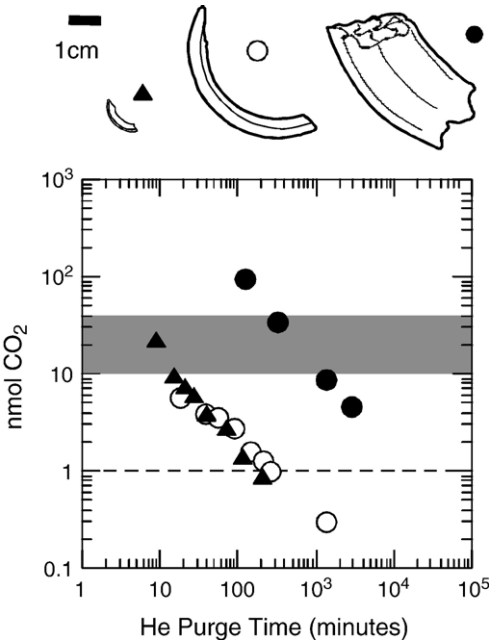

Fig. 2. Rate of CO_2 outgassing from teeth as a function of time elapsed since samples were loaded into the He-purged sample chamber. *Y*-axis shows the amount of CO_2 outgassed per 210 s trapping period. Scale drawings of teeth used in this experiment are, from left to right, Arg2002-46 (fossil rodent incisor), MA-A-V11-20-04 (modern marmot lower incisor), and UCMP 140464 (fossil horse third upper molar). Gray zone indicates the target sample size for CO_2 generated during laser-ablation analysis, and dashed line indicates the maximum permissible rate of CO_2 outgassing during analysis. The marmot and rodent incisors were ready for analysis after ~4 h in the sample chamber, whereas >1 week would have been required to bring the blank to a sufficiently low level for analysis of the horse tooth.

even if the initial blank level was very low following vacuum treatment. This is because the samples reacquire CO_2 during the course of an analytical run, with the new CO_2 coming from laser ablation events and injection of CO_2 standards. This absorption of CO_2 onto the previously CO_2-free sample surfaces leads a to progressive increase in the blank size during an analytical run, and often results in isotopic fractionations of several per mil for both carbon and oxygen.

Analyzing CO_2 standards injected upstream or downstream of the sample chamber identified isotopic fractionation owing to interactions between CO_2 and active sample surfaces. Upstream standards interact with samples prior to leaving the sample chamber, while downstream standards never interact with samples. Upstream standards were fractionated by several per mil for certain samples, especially large samples, and those with significant amounts of adhering bone or sediment matrix.

In general we find that laser ablation using cryofocusing and a capillary GC column is well suited for

the analysis of small, rodent-sized teeth, but is rather poorly suited for analysis of large teeth such as ungulate molars because of high background CO_2 signals and CO_2–sample surface interactions.

3.2. Isotopic response and ablation pit sizes at different laser settings

We repeatedly analyzed a fragment of tooth enamel from a modern black rhinoceros (K00-AB-302p4.2) using laser power settings varying between 2.1 and 21 W, and laser durations of 8.5 ms, and 50 through 500 ms shot duration (our laser system is not capable of producing shots between 8.5 and 50 ms duration). Isotopic zoning within teeth might compromise the meaningful results of experiments investigating the isotopic effect of laser energy, and this fragment was selected because other fragments from the same tooth had been observed to be relatively homogeneous with respect to stable isotopes.

Isotope ratios varied with both laser duration and power. Carbon isotope ratios for 8.5 ms averaged −13.3± 0.1‰ (PDB, 1 σ), −12.7±0.1‰, −12.5±0.1‰, and −12.8±0.3‰ for 2.1, 5.3, 10.5, and 21 W settings,

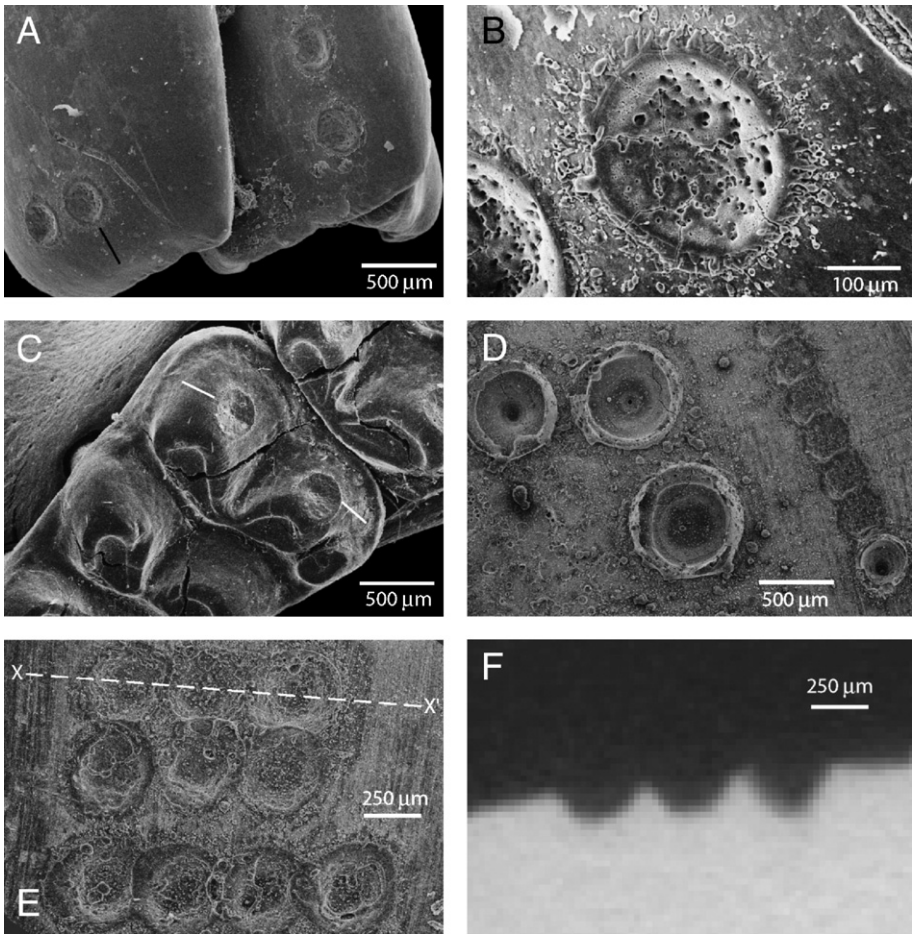

Fig. 3. SEM and X-ray microCT images of laser ablation pits. (A) SEM image of a fossil rodent molar with ablation pits generated at 5.3 W and 8.5 ms. (B) Magnified view of the ablation pit indicated by the line in (A). The surface of the ablation pit is fragile phosphatic glass that condensed from melted apatite following laser ablation. (C) SEM image of a modern rodent molar with ablation pits generated at 5.3 W and 8.5 ms. (D) SEM image of modern rhinoceros enamel (K00-AB-302p4.2) showing three large pits generated at 5.3 W and (upper left to lower center) 50 ms, 85 ms, and 100 ms (e.g. settings similar to those used by Cerling and Sharp, 1996). Medium size pit (lower right) was generated by several consecutive 8.5 ms shots at 5.3 W. Each pit in the string of small pits (right) was generated at 5.3 W and 8.5 ms. The entire sample surface is covered in condensed phosphatic glass spherules (from post-ablation fallout), and melt rings and dark alteration halos surround the large pits. (E) Sets of six (upper) and four (lower) ablation pits in the modern rhinoceros enamel, each typical of the number and arrangement of ablation pits generated for a single isotopic determination. Laser settings are 8.5 ms and 12.5 W (upper six), and 21 W (lower four). Position of the cross-section in (F) is indicated by X-X′. (F) Cross-section through three ablation pits provided by 20-µm-resolution X-ray microCT analysis. Light pixels indicate high density enamel, and dark pixels represent empty space above the sample. SEM images courtesy Ed King, and microCT image courtesy C.L. Lin.

respectively. The isotopic differences between 5.3, 10.5, and 21 W are statistically indistinguishable (*t*-test, Tukey's test, $\alpha = 0.05$), whereas the 2.1 W values differ significantly from all other values. Carbon isotope ratios for 50–500 ms shots averaged -13.2 ± 0.1, and were statistically different from all 8.5 ms power settings except 2.1 W.

Oxygen isotope ratios for 8.5 ms shots were 21.7± 0.4‰ (SMOW, 1σ), 22.2±0.2‰, 22.2±0.1‰, and 21.9±0.2‰ for 2.1, 5.3, 10.5, and 21 W settings, respectively. *T*-tests resolve differences between 2.1 W and 5.3 W, and between 2.1 W and 10.5 W. Tukey's test does not indicate significant differences between the different power settings. Oxygen isotope ratios for 50–500 ms shots averaged 23.4±0.7‰, were significantly different from oxygen isotope ratios generated at 8.5 ms, and showed a significant trend of increasing values with increasing laser energy.

Fig. 3 shows examples of ablation pits on different teeth generated with different laser settings. Fig. 3D shows the relatively large ablation pits associated with the laser settings specified by Cerling and Sharp (1996), while the other images show smaller ablation pits generated with 8.5 ms shots between powers of 5.3 and 21 W. As part of the isotope/laser energy experiment outlined above, we also measured pit depth, diameter, and volume as a function of laser energy. For 8.5 ms shots with powers between 2 and 21 W, diameters ranged between 240 and 300 μm, depths ranged between 70 and 120 μm, and volumes ranged between 0.0016 and 0.0039 mm^3. For the 'long' ablation events (50–500 ms) similar to those used by Cerling and Sharp (1996), but with lower power (5.3 W), ablation pits were significantly larger and had large thermal-alteration melt halos (Fig. 3D). Inclusive of the zones of obvious thermal alteration, diameters ranged between 360 and 480 mm, depths ranged between 200 and 320 mm, and volumes ranged between 0.019 and 0.038 mm^3. We were not able to analyze samples using the long duration and high power (14 W) combination utilized in Cerling and Sharp (1996) because this resulted in even larger pits and production of too much CO_2 for our system.

CO_2 yield per ablated volume of enamel is plotted in Fig. 4 and averaged 1072±125 nmol/mm^3 and 971± 118 nmol/mm^3 for 8.5 ms and 50–500 ms durations, respectively. These values are 75% (8.5 ms) and 68% (50–500 ms) of the theoretical maximum CO_2 yield per volume (1430 nmol/mm^3), and suggest that some enamel is not completely decarbonated during laser ablation, or that CO_2 is resorbed during cooling. The difference in yield between 8.5 ms and 50–500 ms durations is marginally insignificant (*t*-test, $p = 0.07$).

The results in this section indicate that the 8.5 ms ablation event is superior both in terms of minimizing ablation pit size, and increasing isotopic reproducibility. For the configuration of our system, between 2 and 8 individual 'shots' are required in order to generate enough CO_2 (>10 nmol) for a single analysis using the 8.5 ms, 5–12 W setting. All subsequent data reported in this paper was generated using these laser settings. The number of shots necessary could theoretically be decreased by decreasing the flow rate of the capillary GC column, thereby increasing the open-split efficiency.

3.3. Isotopic relationship between laser and conventional analysis, and application to intra-tooth profiles

To verify the isotopic results obtained using laser ablation, we analyzed 25 teeth (14 fossil, 11 modern) that were large enough to also analyze using conventional phosphoric acid digestion (McCrea, 1950; Land et al., 1980). The laser data were corrected for blank contamination, and normalized using injected CO_2 standards. The average isotopic offset (and hence correction factor applied to the unknown data) between the injected CO_2 analyzed through the laser system and the accepted value was −0.9‰ for carbon and −0.6‰ for oxygen. The laser and conventional isotopic results are presented in Table 1 and Fig. 5.

For carbon isotopes, there was a 1:1 relationship between values produced using the laser and those produced using conventional methods, and the average

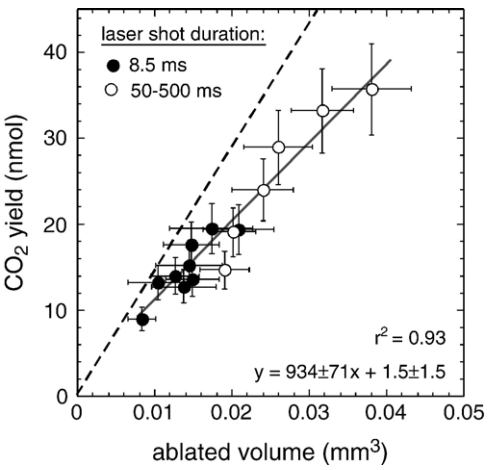

Fig. 4. Bivariate plot showing CO_2 yield as a function of ablated volume. Ablated volume is the total ablation pit volume per analysis, including the volume of melted and density-altered enamel produced during laser ablation. Dashed line shows the theoretical maximum CO_2 yield per volume of enamel, calculated based on the carbonate content per unit volume of enamel.

Table 1
Isotopic comparison between conventional H_3PO_4 analysis and laser-ablation analysis

Sample ID	Taxon, tooth, age (10^6 years)	Conventional H_3PO_4 analysis						Laser ablation analysis						Laser versus conventional			
		n days[a]	*n* analyses[b]	$\delta^{13}C$ (PDB)	±	$\delta^{18}O$ (SMOW)	±	*n* days[a]	*n* analyses[b]	$\delta^{13}C$ (PDB)	±	$\delta^{18}O$ (SMOW)	±	$\varepsilon^*_{las\text{-}conv}$ ($^{13}C/^{12}C$)	±	$\varepsilon^*_{las\text{-}conv}$ ($^{18}O/^{16}O$)	±
Fossil teeth																	
Arg2002-23	Rodent, incisor, 6	1	1	−8.6		27.4		1	1	−9.6		20.5		−1.0	0.4	−6.8	0.4
Arg2002-24	Ungulate, unkn, 6	1	1	−8.9		29.2		1	4	−8.8	0.3	23.3	0.1	0.1	0.2	−5.7	0.4
Arg2002-26	Rodent, incisor, 5	2	4	−2.9	0.1	29.7	1.0	2	5	−4.3	1.2	25.5	0.6	−1.4	1.2	−4.1	1.1
Arg2002-28	Notoungulate, unkn, 4	2	4	−8.9	0.5	28.1	0.6	1	3	−8.0	0.3	22.6	0.1	0.9	0.5	−5.4	0.6
Arg2002-32	Rodent, incisor, 8	2	3	−11.3	0.6	28.3	2.2	1	5	−11.5	0.9	23.1	1.1	−0.2	1.1	−5.1	2.5
Arg2002-33	Rodent, unkn, 8	2	5	−10.3	0.3	25.0	0.5	2	7	−10.4	0.4	19.8	0.3	−0.1	0.4	−5.0	0.6
Arg2002-53	Unknown, 8	2	2	−11.0	0.6	34.9	1.2	1	3	−11.0	0.4	32.0	0.6	0.0	0.7	−2.7	1.3
Arg2002-7	Rodent, incisor, 5	2	2	−5.5	0.5	30.3	0.4	1	3	−6.0	0.7	26.4	0.0	−0.5	0.9	−3.7	0.4
Arg2002-9	Rodent, incisor, 5	2	4	−6.6	0.5	26.8	0.6	1	3	−7.2	0.3	21.5	0.7	−0.6	0.6	−5.2	1.0
IMNH 19001	Proboscidean, molar, 3	2	3	−10.9	0.2	19.8	1.1	2	6	−11.7	0.5	13.8	0.7	−0.8	0.6	−5.9	1.3
Loth 61 L2	Proboscidean, molar, 4	2	4	0.0	0.2	28.0	0.2	1	4	−1.5	0.2	21.0	0.6	−1.5	0.3	−6.8	0.7
SH 15751	Rhino, molar, 8	2	4	−2.5	0.5	29.5	0.5	2	11	−3.5	0.7	25.8	0.5	−0.9	0.8	−3.6	0.7
UNSM 122041	Equid, molar, 6	1	2	−8.7	0.0	21.6	0.6	1	3	−10.4	0.2	14.8	0.1	−1.7	0.2	−6.6	0.6
UNSM 4220	Equid, molar, 7	1	1	−9.0		27.0		1	3	−8.6	1.4	21.6	0.3	0.4	0.2	−5.2	0.4
			Averages:		0.4		0.8				0.6		0.4	−0.5		−5.1	
														0.8 (1σ)		1.2 (1σ)	
Modern teeth																	
Beta ldi1	Goat, incisor	2	3	−12.3	0.6	16.0	1.0	3	19	−10.9	1.4	9.8	0.6	1.4	1.5	−6.2	1.2
Beta ldP2	Goat, premolar	1	2	−7.5	2.5	17.2	1.8	2	8	−6.4	0.7	10.8	0.3	1.1	2.6	−6.2	1.8
CRF ODOC1-p4	Deer, premolar	2	4	−13.7	0.5	24.8	0.3	1	4	−15.0	0.3	17.2	0.3	−1.4	0.5	−7.4	0.5
Epsilon ldi1	Goat, incisor	2	2	−12.4	0.2	16.6	0.6	1	13	−12.6	1.3	8.9	1.1	−0.2	1.3	−7.6	1.2
K00-AB-302p4.1	Rhino, premolar	5	15	−12.7	0.2	28.7	0.5	8	47	−13.4	0.5	22.9	0.4	−0.7	0.6	−5.6	0.6
K01-LAI-218.p1	Impala, unkn	1	2	−5.3	0.0	31.3	0.2	2	10	−6.2	0.5	24.7	0.4	−0.9	0.5	−6.4	0.4
K01-LAI-224.p1	Eland, unkn	1	2	−10.8	0.0	34.1	0.2	1	11	−11.9	0.4	27.2	0.4	−1.2	0.4	−6.7	0.4
K01-LAI-235.p1	Waterbuck, unkn	1	2	1.2	0.1	36.4	0.2	1	11	−0.3	0.7	29.7	1.0	−1.6	0.7	−6.5	1.0
MA-A-11-V11-04	Marmot, molar	2	3	−14.2	0.4	29.5	0.5	1	3	−14.3	0.2	22.4	0.2	0.0	0.5	−6.9	0.5
MA-A-20-V11-04	Marmot, molar	1	1	−11.9		32.5		1	3	−12.7	0.3	26.3	0.2	−0.8	0.2	−6.0	0.4
RRMC1.1	Horse, incisor	1	2	−13.8	0.0	20.8	0.0	1	11	−12.4	0.4	15.4	1.1	1.3	0.4	−5.3	1.1
			Averages:		0.5		0.5				0.6		0.5	−0.3		−6.4	
														1.1 (1σ)		0.7 (1σ)	

±: values are 1σ for δ-values, and propagated error for ε-values. unkn, unknown.

[a] Number of different days the sample was analyzed.

[b] Total number of analyses.

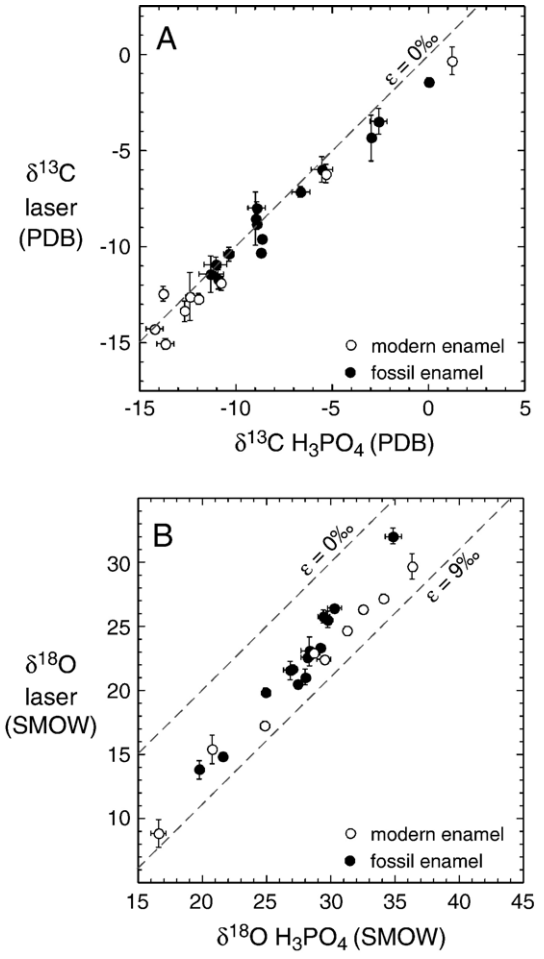

Fig. 5. Comparison between laser and conventional H_3PO_4 analysis. Each data point represents the average and standard deviation (error bars) of laser and conventional analyses of a single tooth. (A) Carbon isotope ratios. Dashed line is a 1:1 line (not a regression line) showing the case where there is no difference between laser and conventional values. The slopes of regression lines through the data are not significantly different from 1. The average offset between laser and conventional analyses is -0.5 ± 0.8 (1σ) and -0.3 ± 1.1‰ for modern and fossil teeth. (B) Oxygen isotope ratios. Dashed lines are 1:1 lines showing where data would plot if laser values were equivalent to CO_3 values ($\varepsilon=0$‰), or if they were equivalent to bulk enamel values (~equal to PO_4 values; $\varepsilon=-9$‰). The average offset between laser and conventional analysis is -5.1 ± 1.2‰ and -6.4 ± 0.7‰ for fossil and modern enamel. The slopes of regression lines through the data are not significantly different from 1.

offset, expressed as $^{13}\varepsilon*_{\text{laser-acid}}$ was -0.5 ± 0.8‰ (1σ) for fossil enamel, and -0.3 ± 1.1‰ for modern enamel. This difference is not significant (t-test, $p=0.26$), demonstrating that modern enamel is suitable for carbon isotope analysis using laser ablation, despite the fact that it may typically have a higher organic fraction than fossil enamel.

For oxygen isotopes, there was also a 1:1 relationship between laser and conventional isotope ratios. The average offset was -5.1 ± 1.2‰ for fossil enamel, and -6.4 ± 0.7 ‰ for modern enamel; this difference is significant (t-test, $p=0.002$). $^{18}\varepsilon*_{\text{laser-acid}}$ values ranged between -2.7‰ and -7.6‰, and were significantly more variable than for carbon. Modern enamel shows a higher degree of oxygen isotope reproducibility than fossil enamel, and is well suited for oxygen isotope analysis using laser ablation.

We also measured intra-tooth isotopic variation in three different modern teeth: an upper incisor from a marmot collected in the mountains of Utah (Maple Canyon), a lower incisor from a marmot collected in Mongolia, and an upper incisor from a rabbit that underwent a controlled dietary switch. The enamel thickness for the rabbit upper incisor measured using X-ray microCT is 100 ± 20 μm. A lower incisor from the same rabbit has been analyzed using the H_3PO_4 method (Passey et al., 2005), and we present these results for comparison. The enamel of the marmot incisors was coated with a natural iron-containing pigment typical of many rodents, and this was abraded away using a low speed drill prior to analysis because previous lasing of similar material on different teeth resulted in production of black halos possibly resulting from charring of organic material.

The intra-tooth isotope profiles are shown in Fig. 6. The marmots from Utah and Mongolia (Fig. 6A and B) show quasi-sinusoidal isotopic variation and have respective isotope amplitudes of 7.1‰ and 8.2‰ for oxygen, and 3.4‰ and 3.8‰ for carbon. In both incisors, the carbon isotope minima correspond spatially with disruptions in enamel morphology similar to 'hibernation marks' described in squirrels and marmots (Rinaldi, 1999; Goodwin et al., 2005). Carbon isotope depletion in the tooth enamel is consistent with utilization of ^{13}C-depleted lipids as a primary energy source during hibernation (Vogel, 1978), and therefore these profiles may record the isotopic signature of hibernation. Oxygen isotopes are consistent with this scenario, showing relatively ^{18}O-depleted enamel that coincides with depletions in ^{13}C and positions of the putative hibernation marks.

The rabbit whose incisor intra-tooth isotope profiles are depicted in Fig. 6C and D was an experimental animal that was maintained on a C_3 feed (alfalfa, $\delta^{13}C=-27.3$‰), then given a 21-day dietary switch to a C_4-based feed (corn-based pellets, $\delta^{13}C=-17.2$‰), and finally switched back to the C_3 feed; details of this experiment are given in Passey et al. (2005). Fig. 6C shows isotopic results from an upper incisor measured using the laser system, whereas Fig. 6D shows results from a lower incisor measured using the conventional H_3PO_4 method. The lower incisor is larger than the upper incisor and is at the extreme limit of

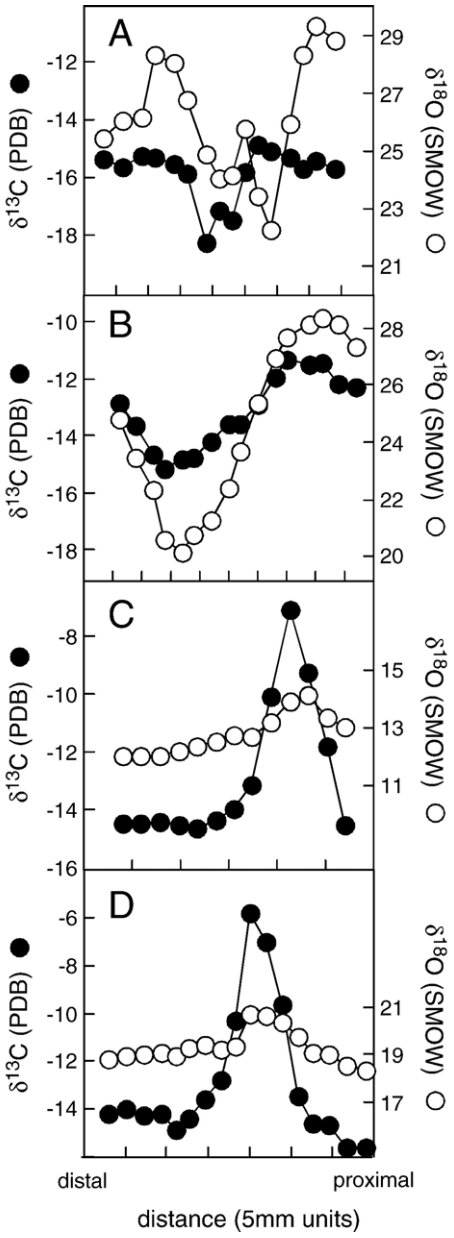

Fig. 6. Intra-tooth isotope profiles measured using the laser system. (A) Upper incisor of a marmot collected in Utah. (B) Lower incisor of a marmot collected in Mongolia. Carbon-isotope minima in both (A) and (B) coincide with growth-marks in the enamel that are similar to 'hibernation marks' reported in the literature (Goodwin et al., 2005). (C) Upper incisor of an experimental animal (rabbit) that was equilibrated to a C_3 diet, changed to C_4 feed for 21 days, and then switched back to C_3 feed. (D) Conventionally-measured (H_3PO_4) isotope profile from a lower incisor of the same animal in (C).

what is possible to analyze using conventional methods. The two profiles show essentially the same pattern, with minor differences that are expected because of the slightly different growth rates of the teeth.

4. Discussion and conclusions

The results presented here show a significant reduction in ablation pit size compared to earlier studies (e.g. Cerling and Sharp, 1996), while maintaining similar accuracy and precision. Of specific relevance to analysis of tooth enamel is the depth of ablation pits, because pits that are too deep penetrate into underlying dentine. Dentine contains organic compounds that interfere with mass spectrometry, either directly as isobaric interferences, or by being oxidized to CO_2 during laser ablation and thus contaminating the enamel-derived CO_2 sample. We have shown that ablation pits less than ~100 μm deep can be achieved using very short pulses of low power 10.6 μm laser radiation, and that teeth can be reliably analyzed using these laser settings, especially when gas from several ablation events is pooled for analysis. In their study, Cerling and Sharp (1996) estimate pit depths of ~650 mm, with pits tunneling into the underlying dentine in some ungulate teeth (e.g. Cerling and Sharp, 1996, Fig. 3). Experimentation in our lab using similar laser settings shows that the thermally altered zone can actually penetrate as much as 1 mm below the surface of the enamel. The six-fold or greater reduction in pit depth achieved by this study has important ramifications for analysis of small mammal tooth enamel, because more than 75% of terrestrial mammal species have body masses less than 1.2 kg (Blackburn and Gaston, 1998), and mammals of this size rarely have enamel exceeding a few hundred microns in thickness.

Carbon isotope ratios observed using this method are typically within about 1‰ of the number obtained by conventional phosphoric acid digestion. The level of precision is variable and appears to depend on the homogeneity of the sample being analyzed, as was suggested by Cerling and Sharp (1996). For example, the average standard deviation for the analyses reported in Table 1 is 0.6‰, but for the rabbit incisor shown in Fig. 6C, the standard deviation of the distal 5 samples representing the time when the animal was eating an isotopically homogeneous C_3 diet is less than 0.1‰.

The precision and accuracy of carbon isotope analysis using this method is appropriate for many applications involving dietary reconstruction. Carbon isotope ratios in mammals are most commonly used to differentiate between C_3 and C_4 diets. The isotopic difference between these two plant types is ~14‰, so the laser method will easily distinguish C_3 and C_4 feeders, but with a conservative uncertainty of ~20% (3.2‰ 2σ range/14‰) in the exact ratio of the two food types. The method will also be suitable for studying intra-tooth

variation, where relative changes, as opposed to absolute values, are more important.

Accuracy of oxygen isotope data produced using this method is lower than that realized for conventional methods and most other laser methods. For fossil enamel, $^{18}\varepsilon^{*}_{\text{laser-conv}}$ values range between −2.7‰ and −6.8‰, and for modern enamel it ranges between −5.3‰ and −7.6‰. The greater variability for fossil enamel compared to modern enamel may be related to the fact that laser ablation samples bulk enamel, which in fossils may be contaminated with diagenetic oxygen-bearing phases (Kohn et al., 1999), and which may undergo a variable diagenetic decrease in the isotopic spacing between the PO_4 and CO_3 components of the mineral (Iacumin et al., 1996; Zazzo et al., 2004), and replacement of OH^- with F^-. A decrease in the PO_4–CO_3 spacing would have the effect of lowering the magnitude of $^{18}\varepsilon^{*}_{\text{laser-conv}}$ values, which is consistent with our results for fossil versus modern samples. Such diagenesis would affect the results of not only this laser method, but also any other that also samples bulk enamel.

As outlined in previous studies (Cerling and Sharp, 1996; Kohn et al., 1996; Jones et al., 1999; Sharp et al., 2000), the oxygen isotope offset between laser and conventional analysis should partially depend on the completeness of mixing of oxygen-bearing phases in apatite during ablation events. According to the stoichiometry of Elliott (1997), 91.5% of the oxygen in enamel bioapatite occurs in phosphate, 5.6% in carbonate, and 2.9% in hydroxide. The 'apparent' fractionation between oxygen in PO_4 and CO_3 is ~9‰ for modern bioapatite (Bryant et al., 1996; Iacumin et al., 1996) ('apparent' because the oxygen isotope fractionation between H_3PO_4-liberated CO_2 and mineral apatite CO_3 is unknown, but is assumed to be the same as that observed for calcite), with CO_3 being the ^{18}O-enriched phase. The fractionation between OH and the other oxygen-bearing phases is unknown, but has been indirectly estimated by Jones et al. (1999) to be −16.6‰ relative to PO_4. For complete oxygen mixing during laser ablation, the δ^{18}O value of laser-generated CO_2 should be equal to the δ^{18}O value of bulk tooth enamel. Using the parameters listed above, the bulk value of tooth enamel should be 9.0‰ depleted relative to the CO_3 value, with a minimum value of ~8.0‰ in the case of very high CO_3 content or a more positive actual fractionation between OH and PO_4. Therefore, the expected value for $^{18}\varepsilon^{*}_{\text{laser-conv}}$ in the case of complete oxygen mixing during laser ablation is −8‰ to −9‰.

Our $^{18}\varepsilon^{*}_{\text{laser-conv}}$ values are not only lower than this predicted value, but they differ between fossil and modern enamel, and differ from the value of −7.0± 1.4‰ observed by Cerling and Sharp (1996). We cannot account for the difference between this study and Cerling and Sharp (1996), but it may be related to several factors, including different calibration and correction procedures, analysis of different samples with different diagenetic histories, and utilization of different laser parameters.

The lower magnitude of $^{18}\varepsilon^{*}_{\text{laser-conv}}$ values compared to expected values for bulk enamel might reflect incomplete mixing of oxygen-bearing phases and bias towards oxygen from the carbonate phase (although the signal is still dominated by phosphate oxygen). In many but not all diagenetic environments, the carbonate component of bioapatite appears to be more susceptible to isotopic alteration than does the phosphate component (Zazzo et al., 2004). Therefore, δ^{18}O data obtained using these methods on fossil enamel can be biased by diagenetic effects, and methods targeting phosphate oxygen may be a better alternative (Lindars et al., 2001; Grimes et al., 2003) when carbonate-component alteration is suspected.

In summary, the laser ablation methods described in this paper are not ideal for oxygen isotope applications requiring the highest possible accuracy and precision, such as those seeking to reconstruct the absolute isotopic composition of body water within a few tenths of a per mil. However, the high degree of correlation between conventional and laser δ^{18}O values (Fig. 5) shows that the primary signal exists, and that the method is capable of resolving large-scale differences in δ^{18}O. The intra-tooth results shown in Fig. 6 are not particularly 'noisy', suggesting that high precision of δ^{18}O analysis is possible for pristine teeth. The pattern of oxygen isotope variation in the rabbit incisor analyzed by laser ablation (Fig. 6C) is similar to that analyzed using the phosphoric method (Fig. 6D), suggesting that the degree of mixing between different oxygen-bearing components of enamel is similar for multiple analyses of the same tooth. Therefore, the method will likely be useful for revealing intra-tooth and intra-individual variation, and for studying large-scale environmental gradients.

This paper shows that background CO_2 contamination is a significant problem when analyzing large samples, and must also be considered when analyzing small samples. For example, carbon isotope blank corrections for the data presented in Table 1 (small samples) ranged between −0.4‰ and +1.0‰. The blank correction is a function of blank size, blank isotopic composition, sample size, and sample isotopic composition, so each analysis is subject to a unique blank correction based on mass balance calculations. Related to the background contamination is isotopic fractionation associated with

interactions of sample CO_2 with the surfaces of tooth samples. This problem increases as a function of increasing sample size, and along with the background problem prevents large samples from being successfully analyzed. The effect can be as high as several per mil for both carbon and oxygen, but for the 'small' samples reported in Table 1, correction factors based on the observed value of CO_2 standards injected upstream of the sample chamber are still significant, averaging −0.9‰ for carbon and −0.6‰ for oxygen.

This method is therefore best suited to the analysis of small teeth (or small tooth fragments). Small mammals are abundant, both in terms of species richness and numbers of individuals. They are well preserved in the fossil record and are the basis for detailed biostratigraphies. In terms of paleoenvironmental reconstruction, small mammals have enormous potential as paleoenvironmental archives. Isotope systematics in animals systems are complex and rely heavily on empirical calibrations using modern, free-living animals. Unfortunately, pristine ecosystems are becoming exceedingly rare for large animals with large wandering-ranges. On the other hand, small mammals such a rodents can live entire lives within very small parcels of land that are essentially pristine. Because small mammals do not typically move large distances, those sampled at high elevation, low elevation, in forests, or in grasslands will reflect the isotopic signature of those specific environments. Isotopic calibration is therefore more feasible for these animals, in terms of logistics and meaningfulness of data. The methods presented in this paper, while certainly not the end-all for carbon and oxygen isotopic analysis of small animals, provide a means for beginning the development of an isotopic framework for this important group of animals.

In summary, this paper has shown that useful carbon and oxygen isotopic measurements can be made using laser ablation on teeth with enamel as thin as ~100 um. The key steps necessary to achieve this are: (1) using a medium power (~5–15 W) CO_2 laser with a short pulse duration (<10 ms), (2) analyzing CO_2 pooled from several separate laser ablation events (each corresponding to a different ablation pit) and cryofocusing CO_2 generated from these in a liquid nitrogen trap prior to introduction into a capillary GC column, (3) measurement of, and correction for, background CO_2 contamination, and (4) system behavior monitoring and isotopic corrections using syringe-injected carbon dioxide standards. Analysis of intra-tooth variation in irregularly shaped teeth is made possible by using a rotating sample mount chamber (Fig. 1), and modern enamel may be analyzed with similar or higher accuracy and precision than fossil enamel.

Acknowledgements

We thank the following individuals who were involved in different stages of the development of these methods: Linda Ayliffe, David Fox, Scott Hynek, Naomi Levin, Jackie Rabb. We thank Matt Sponheimer for providing the initial impetus to resurrect the laser system, and Scott Hynek for help with analyzing the Argentina fossil teeth. We thank Jim Ehleringer and Craig Cook for facilities support, Ed King for the SEM images, and C.L. Lin for the microCT data. Michael Rosenmeier and Marion Sikora provided the Mongolia marmot incisor. BHP thanks Zach Sharp for an introduction to the laser ablation system at the University of New Mexico. We thank Stephen Grimes for providing a useful review. This work was partially supported by the National Science Foundation.

References

Blackburn, T.M., Gaston, K.J., 1998. The distribution of mammal body masses. Diversity and Distributions 4, 121–133.

Bryant, J.D., Koch, P.L., Froelich, P.N., Showers, W.J., Genna, B.J., 1996. Oxygen isotope partitioning between phosphate and carbonate in mammalian apatite. Geochimica et Cosmochimica Acta 60, 5145–5148.

Cerling, T.E., Sharp, Z.D., 1996. Stable carbon and oxygen isotope analysis of fossil tooth enamel using laser ablation. Palaeogeography, Palaeoclimatology, Palaeoecology 126, 173–186.

Elliott, J.C., 1997. Structure, crystal chemistry and density of enamel apatites. In: Chadwick, D.J., Cardew, G. (Eds.), Dental Enamel. John Wiley & Sons, Chichester, pp. 54–67.

Goodwin, H.T., Michener, G.R., Gonzalez, D., Rinaldi, C.E., 2005. Hibernation is recorded in lower incisors of recent and fossil ground squirrels (Spermophilus). Journal of Mammalogy 86, 323–332.

Grimes, S.T., Mattey, D.P., Hooker, J.J., Collinson, M.E., 2003. Paleogene paleoclimate reconstruction using oxygen isotopes from land and freshwater organisms: the use of multiple paleoproxies. Geochimica et Cosmochimica Acta 67, 4033–4047.

Iacumin, P., Bocherens, H., Mariotti, A., Longinelli, A., 1996. Oxygen isotope analyses of co-existing carbonate and phosphate in biogenic apatite: a way to monitor diagenetic alteration of bone phosphate? Earth and Planetary Science Letters 142, 1–6.

Jones, A.M., Iacumin, P., Young, E.D., 1999. High-resolution $\delta^{18}O$ analysis of tooth enamel phosphate by isotope ratio monitoring gas chromatography mass spectrometry and ultraviolet laser fluorination. Chemical Geology 153, 241–248.

Koch, P.L., 1998. Isotopic reconstruction of past continental environments. Annual Review of Earth and Planetary Sciences 26, 573–613.

Kohn, M.J., Cerling, T.E., 2002. Stable isotope compositions of biological apatite. Phosphates: Geochemical, Geobiological, and Materials Importance 48, 455–488.

Kohn, M.J., Schoeninger, M., Valley, J., 1996. Herbivore tooth oxygen isotope compositions: effects of diet and physiology. Geochimica et Cosmochimica Acta 60, 3889–3896.

Kohn, M.J., Schoeninger, M.J., Barker, W.W., 1999. Altered states: effects of diagenesis on fossil tooth chemistry. Geochimica et Cosmochimica Acta 63, 2737–2747.

Land, L.S., Lundelius, E.L., Valastro, S., 1980. Isotopic ecology of deer bones. Palaeogeography, Palaeoclimatology, Palaeoecology 32, 143–151.

Lecuyer, C., 2004. Oxygen isotope analysis of phosphate. In: de Groot, P.A. (Ed.), Handbook of Stable Isotope Analytical Techniques, vol. 1. Elsevier, pp. 482–499.

Lindars, E.S., et al., 2001. Phosphate $\delta^{18}O$ determination of modern rodent teeth by direct laser fluorination: an appraisal of methodology and potential application to palaeoclimate reconstruction. Geochimica et Cosmochimica Acta 65, 2535–2548.

Longinelli, A., 1984. Oxygen isotopes in mammal bone phosphate: a new tool for paleohydrological and paleoclimatological research? Geochimica et Cosmochimica Acta 48, 385–390.

McCrea, J.M., 1950. On the isotope chemistry of carbonates and a paleotemperature scale. The Journal of Chemical Physics 18, 849–857.

O'Neil, J.R., Roe, L.J., Reinhard, E., Blake, R.E., 1994. A rapid and precise method of oxygen isotope analysis of biogenic phosphate. Israel Journal of Earth Science 43, 203–212.

Passey, B.H., et al., 2005. Inverse methods for estimating primary input signals from time-averaged isotope profiles. Geochimica et Cosmochimica Acta 69, 4101–4116.

Rinaldi, C., 1999. A record of hibernation in the incisor teeth of Recent and fossil marmots (*Marmota flaviventris*). In: Mayhall, J. (Ed.), 11th International Symposium on Dental Morphology. Oulu University Press, Oulu, Finland, pp. 112–119.

Sharp, Z.D., Cerling, T.E., 1996. A laser GC-IRMS technique for in situ stable isotope analyses of carbonates and phosphates. Geochimica et Cosmochimica Acta 60, 2909–2916.

Sharp, Z.D., Cerling, T.E., 1998. Fossil isotope records of seasonal climate and ecology: straight from the horse's mouth. Geology 26, 219–222.

Sharp, Z.D., Atudorei, V., Furrer, H., 2000. The effect of diagenesis on oxygen isotope ratios of biogenic phosphates. American Journal of Science 300, 222–237.

Vennemann, T.W., Fricke, H.C., Blake, R.E., O'Neil, J.R., Colman, A., 2002. Oxygen isotope analysis of phosphates: a comparison of techniques for analysis of Ag_3PO_4. Chemical Geology 185, 321–336.

Vogel, J.C., 1978. Isotopic assessment of the dietary habits of ungulates. South African Journal of Science 74, 298–301.

Zazzo, A., Lecuyer, C., Sheppard, S.M.F., Grandjean, P., Mariotti, A., 2004. Diagenesis and the reconstruction of paleoenvironments: a method to restore original $\delta^{18}O$ values of carbonate and phosphate from fossil tooth enamel. Geochimica et Cosmochimica Acta 68, 2245–2258.